Available online at www.sciencedirect.com

ScienceDirect

Neuromuscular Disorders 32 (2022) 15–24

www.elsevier.com/locate/nmd

Diaphragmatic dysfunction in neuromuscular disease, an MRI study

Laurike Harlaar[a,f], Pierluigi Ciet[b,c], Gijs van Tulder[b], Esther Brusse[a], Remco G.M. Timmermans[d], Wim G.M. Janssen[d], Marleen de Bruijne[b,e], Ans T. van der Ploeg[f], Harm A.W.M. Tiddens[b,c], Pieter A. van Doorn[a], Nadine A.M.E. van der Beek[a,*]

[a] *Erasmus MC, University Medical Center Rotterdam, Center for Lysosomal and Metabolic Diseases, Department of Neurology, Rotterdam, the Netherlands*
[b] *Erasmus MC, University Medical Center Rotterdam, Department of Radiology and Nuclear Medicine, Rotterdam, the Netherlands*
[c] *Erasmus MC – Sophia Children's Hospital, University Medical Center Rotterdam, Department of Respiratory Medicine and Allergology, Rotterdam, the Netherlands*
[d] *Rijndam Rehabilitation Centre Rotterdam, location Erasmus MC, Rotterdam, the Netherlands*
[e] *University of Copenhagen, Department of Computer Science, Copenhagen, Denmark*
[f] *Erasmus MC – Sophia Children's Hospital, University Medical Center Rotterdam, Center for Lysosomal and Metabolic Diseases, Department of Paediatrics, Rotterdam, the Netherlands*

Received 17 March 2021; received in revised form 3 September 2021; accepted 2 November 2021

Abstract

The aim of this exploratory study was to evaluate diaphragmatic function across various neuromuscular diseases using spirometry-controlled MRI. We measured motion of the diaphragm relative to that of the thoracic wall (cranial-caudal ratio *vs.* anterior posterior ratio; CC-AP ratio), and changes in the diaphragmatic curvature (diaphragm height and area ratio) during inspiration in 12 adults with a neuromuscular disease having signs of respiratory muscle weakness, 18 healthy controls, and 35 adult Pompe patients – a group with prominent diaphragmatic weakness. CC-AP ratio was lower in patients with myopathies (n=7, 1.25±0.30) and motor neuron diseases (n=5, 1.30±0.10) than in healthy controls (1.37±0.14; p=0.001 and p=0.008), but not as abnormal as in Pompe patients (1.12±0.18; p=0.011 and p=0.024). The mean diaphragm height ratio was 1.17±0.33 in patients with myopathies, pointing at an insufficient diaphragmatic contraction. This was also seen in patients with Pompe disease (1.28±0.36), but not in healthy controls (0.82±0.33) or patients with motor neuron disease (0.82±0.24). We conclude that spirometry-controlled MRI enables us to investigate respiratory dysfunction across neuromuscular diseases, suggesting that the diaphragm is affected in a different way in myopathies and motor neuron diseases. Whether MRI can also be used to evaluate progression of diaphragmatic dysfunction requires additional studies.

Keywords: Myopathy; Motor neuron disease; Pompe disease; Respiratory insufficiency; Diaphragm; MRI.

1. Introduction

Respiratory insufficiency is a well-known problem in patients with neuromuscular diseases and has been described in various types of myopathies and in motor neuron diseases [1,2]. This insufficiency can be caused by weakness of the diaphragm, but also by weakness of the intercostal muscles and accessory respiratory muscles [3,4]. Insight in the patterns of respiratory muscle weakness could help to understand the pathophysiology of respiratory insufficiency in different types of neuromuscular disease, and possibly to evaluate the disease course and future treatment effects. While spirometry evaluates overall pulmonary function, MRI can help to specifically study the function of the diaphragm relative to that of the other respiratory muscles [5].

In Pompe disease, a genetic metabolic muscle disease, respiratory insufficiency is caused mainly by a decreased diaphragmatic function [6,7]. Pompe patients showed a decreased downwards diaphragmatic motion and an abnormal

* Corresponding author at: Erasmus MC, University Medical Center Rotterdam, Center for Lysosomal and Metabolic Diseases, Department of Neurology, Dr. Molewaterplein 40, 3015 GD Rotterdam, the Netherlands.
E-mail address: n.beek@erasmusmc.nl (N.A.M.E. van der Beek).

https://doi.org/10.1016/j.nmd.2021.11.001

increased curvature of the diaphragm during inspiration on MRI. Conversely, motion of the thoracic wall, expressed as function of the intercostal muscles, remained within the normal range [8–10]. We recently showed that MRI can be also used to investigate early impairment of the diaphragm in patients with Pompe disease [11]. It is unknown, however, whether these findings are specific for Pompe disease, or whether the diaphragm is affected in a similar way in other types of neuromuscular diseases. Interestingly, it was shown in patients with Duchenne muscular dystrophy that both diaphragmatic motion and thoracic wall motion were decreased [12–14]. Increased knowledge about the involvement of different respiratory muscles across patients with neuromuscular diseases could aid to a better understanding and recognition of the sequence of events that finally lead to respiratory insufficiency, including early signs of diaphragmatic involvement. This information potentially is also relevant for timely therapeutic interventions and studies on treatment effects. MRI might be a useful tool to visualize and quantify the early signs and progression of respiratory muscle weakness.

The aim of this study was to explore the function of the diaphragm relative to that of the intercostal muscles in various types of myopathies and motor neuron disease using MRI.

2. Methods

2.1. Study design and participants

In this cross-sectional exploratory study, patients with various types of neuromuscular disease were recruited at the departments of Neurology and Rehabilitation of Erasmus MC University Medical Center. Inclusion criteria were: a confirmed diagnosis of either a myopathy (other than Pompe disease) or motor neuron disease by a neuromuscular expert; signs of respiratory muscle weakness defined as a vital capacity less than 80% of predicted using spirometry during screening; and the ability to lay flat for at least 30 minutes, in order to undergo MRI examination. Exclusion criteria were severe comorbidities and medical devices, claustrophobia or other general contraindications to MRI. Patients were included consecutively between April 2017 and March 2019. We compared our findings to the results of 35 patients with a DNA-confirmed diagnosis of Pompe disease and 18 healthy controls matched for gender and age to the Pompe patients [11]. The protocol was approved by the Medical Ethical Committee of Erasmus MC University Medical Center (MEC-2007-103, amendment 7). All participants provided written informed consent.

2.2. Pulmonary function tests

All participants started with regular pulmonary function tests, including forced vital capacity (FVC) in upright seated and supine positions and maximum static inspiratory pressure (MIP) and expiratory pressure (MEP) in the upright position. All parameters were expressed as a percentage of predicted normal values [15–17]. In addition, patients were trained to perform specific breathing manoeuvres during MRI scanning. Patients were not excluded when pulmonary function tests results during the day of MRI investigations were slightly better than expected based on spirometry results during screening.

2.3. Image acquisition

MRI images were conducted during a 20-25-minute protocol with a 3 Tesla Signa 750 MRI system (General Electric Healthcare, Milwaukee, Winconsin, USA) using the whole-body coil for radio-frequency excitation and a 32-channel torso coil for signal reception [11]. In the current study, we used three-dimensional (3D) static images acquired at end-inspiration and end-expiration and sagittal two-dimensional (2D) dynamic images at the level of the right mid-hemidiaphragm acquired during forced inspiration. Breathing manoeuvres during MRI were spirometry-controlled to ensure the maximum performance and volume standardization for each patient. We did not include images of the left mid-hemidiaphragm since its segmentation is cumbersome due to the difficult delineation of heart and diaphragm contours [11]. Further, we had no indication for body side predominant involvement of respiratory muscle weakness in any of the patients who participated.

2.4. Image analysis

For image analysis, we developed automatic lung segmentation models using convolutional neural networks based on a 2D or 3D U-Net architecture [18]. The models were implemented and trained with the TensorFlow toolbox for Python (TensorFlow 1.14, https://www.tensorflow.org/, ©2019, The TensorFlow authors; Python 3.6.3, https://www.python.org/, ©2001-2019, Python Software Foundation). The 3D segmentations were based on the full 3D scans and the model was trained on manual lung segmentations in every second axial slice of 10 Pompe patients and 6 healthy controls, using interpolation co complete the unlabelled axial slices [8]. The 2D segmentations were made independently for each frame in the sequence. The same segmentation network was used for the left and right lung. To remove any stray pixels, only the largest object in each segmented image was kept as the final result. The training data included manual segmentations of 18 healthy controls and 35 Pompe patients who also participated in the current study [11]. Data augmentation with elastic deformations was used to extend the training set [18]. Before segmentation, all scans were normalized using the N4ITK bias field correction algorithm [19]. After segmentation, the binary output of the network was post-processed with a morphological hole-filling operation to remove any small holes from the automatic lung segmentations. All lung segmentations produced by the automated models were manually checked for inaccuracies and corrected in case of oversegmentations or scanning

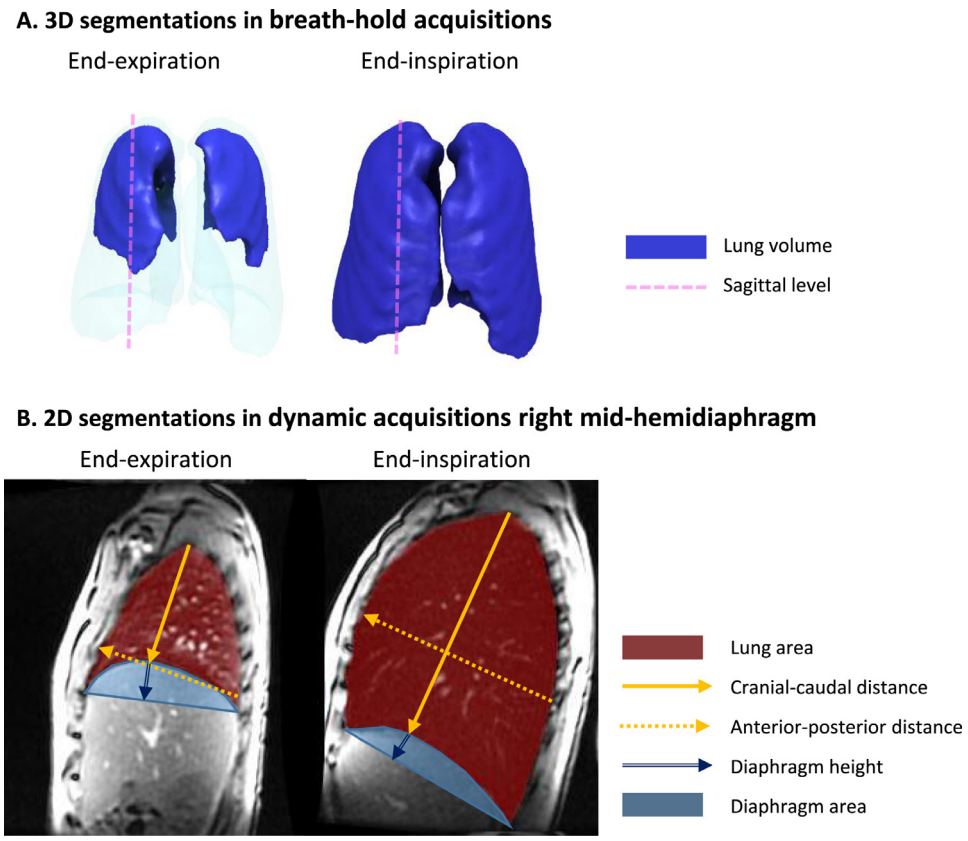

Fig. 1. Outcome measures. Explanation of different outcome measures in an exemplary MRI of a healthy control. A) The lung volume of the three-dimensional (3D) images is derived from the automatic voxelwise segmentation of the lungs. The level of the two-dimensional (2D) sagittal images is indicated. B) For the dynamic 2D images, the automatic pixelwise segmentation for each frame is used to compute the total lung area and other measurements. Cranial-caudal distance is the distance between the lung apex and diaphragm apex. Anterior-posterior distance is the longest distance from the anterior to the posterior side of the lung perpendicular to the cranial-caudal distance. Diaphragm height is the perpendicular distance between the diaphragm apex and the linear line connecting both diaphragm corners. Diaphragm area is the area between the diaphragm contour and the linear line. For analysis, we calculated ratios by dividing the outcomes at end-inspiration by the outcomes at end-expiration to correct for differences in size of the patient.

artefacts. Manual adjustments were made for 6% of the 3D segmentations in healthy controls, 14% of the Pompe patients and 54% of the patients with other myopathies and motor neuron diseases; and for 0% of the 2D segmentations in healthy controls, 1% of the Pompe patients and 39% of the patients with other myopathies or motor neuron diseases. The fact that most adjustments were needed for patients with other myopathies or motor neuron diseases is because the training data included manual segmentations of healthy controls and Pompe patients only.

2.5. MRI outcome measures

To analyse the function of the diaphragm and other respiratory muscles, we calculated seven different MRI parameters. On 3D images, we calculated 1) the lung volume ratio between inspiration and expiration to evaluate the total increase in lung volume during inspiration (Fig. 1A). On sagittal 2D images, we calculated 2) the lung area ratio to evaluate the total increase in lung area during inspiration, 3) the cranial-caudal ratio to evaluate motion of the diaphragm, 4) the anterior-posterior ratio to evaluate motion of the thoracic wall, 5) the ratio between the cranial-caudal ratio and the anterior-posterior ratio to evaluate the relative motion of the diaphragm compared to the motion of the thoracic wall, and 6) the height and 7) area below the diaphragmatic dome to evaluate the curvature of the diaphragm (Fig. 1B). All MRI parameters are ratios, calculated by dividing the outcomes at end-inspiration by the outcomes at end-expiration, to correct for differences in size of the patient.

The analysis was performed using custom-built scripts. The 3D analysis was executed in MATLAB (Mathworks, Natick, MA), by converting the automatic voxelwise segmentation of the lungs into a 3D mesh grid of the lung surface, before computing the measurements [9]. The 2D measurements were computed directly from the binary segmentation using Python (Python 3.6.3, https://www.python.org/, ©2001-2019. Python Software Foundation; SciPy 1.1.0, https://www.scipy.org/, ©2003-2019 SciPy developers).

2.6. Statistical analysis

Patients with several types of myopathies and patients with motor neuron diseases were compared to healthy controls and to Pompe patients. Baseline characteristics and pulmonary function test outcomes were compared between subgroups

Table 1
Participant characteristics.

Baseline characteristics	Myopathies (n=7)	Motor neuron disease (n=5)	Pompe disease (n=35)	Healthy controls (n=18)
Sex, number of males (%)	7 (100%)**,^	3 (60%)	18 (51%)	8 (44%)
Age, years	51 ± 12	67 ± 6**,^^	40 ± 16	43 ± 14
Height, cm	184 ± 7	171 ± 5	176 ± 10	178 ± 12
Weight, kg	83 ± 18	75 ± 19	74 ± 15	79 ± 14
BMI, kg/m^2	25 ± 6	25 ± 5	24 ± 4	25 ± 3
Wheelchair, n (%)	1 (14%)	1 (20%)	1 (3%)	0 (0%)
Non-invasive ventilation, n (%)	1 (14%)	0 (0%)	1 (3%)	0 (0%)
Smokers, n (%)	2 (29%)*	2 (40%)**,^	2 (6%)	0 (0%)
Pulmonary function test outcomes				
FVC upright, % of predicted	79 ± 10**	82 ± 14**	88 ± 13	106 ± 8
FVC supine, % of predicted	76 ± 10**	79 ± 18**	73 ± 20	102 ± 8
Δ FVC, % of predicted	3 ± 4^^	3 ± 16	15 ± 12	4 ± 4
MIP, % of predicted	75 ± 21*	78 ± 35	77 ± 25	106 ± 25
MEP, % of predicted	54 ± 25**,^	87 ± 31	80 ± 27	112 ± 28

Baseline characteristics and pulmonary function tests outcomes of different groups. Continues values are presented as mean ± standard deviation and categorical values are presented as number with percentage. Statistically significant differences between subgroups are indicated:
* $p<0.05$ compared to healthy controls
** $p<0.0125$ compared to healthy controls
^ $p<0.05$ compared to Pompe patients
^^ $p<0.0125$ compared to Pompe patients.
BMI = body mass index, FVC = forced vital capacity, Δ FVC = FVC upright – FVC supine, MIP = maximum inspiratory pressure, MEP = maximum expiratory pressure.

using the chi-square test for categorical variables (sex, number of patients with wheelchair, number of patients with non-invasive ventilation and number of smokers) and the Mann Whitney test for continuous variables (age, height, weight, BMI, and pulmonary function test outcomes). To analyze differences in MRI outcomes, we used multiple linear regression analysis, with the patient group as main factor and significant differences in patient characteristics between subgroups (age, sex and smoking) as covariates. In addition, FVC upright was added as a covariate to exclude a possible effect of the severity of respiratory muscle weakness, instead of the specific neuromuscular type of disease, on the MRI outcomes. Residual plots were inspected to check the linearity assumption.

The Spearman's rank correlation coefficient was used to calculate the strength of association between the pulmonary function test outcomes and the MRI outcomes.

Statistical analysis was performed with SPSS for Windows (version 25, SPSS Inc, Chicago, IL). The significance level was set at $p \leq 0.05$. Differences between groups were corrected for multiple testing using Bonferroni's method, resulting in a significance level of $p \leq 0.0125$ (four comparisons). Due to the exploratory character of the study, we did not adjust for multiple testing when reporting the different MRI outcomes.

3. Results

3.1. Patient characteristics

We included 12 patients with various neuromuscular diseases other than Pompe disease (age range 37-73 years) (Table 1), comprising seven patients with myopathies (nemaline myopathy (n=2), myofibrillar myopathy type 2 (n=1), inclusion body-myositis (n=2) and myotonic dystrophy type 1 (n=2)), and five patients with motor neuron diseases (progressive spinal muscular atrophy (n=3) and amyotrophic lateral sclerosis (n=2)). Compared to healthy controls (n=18) and patients with Pompe disease (n=35), patients with myopathies and motor neuron diseases were older, more often males and more often active smokers (Table 1).

3.2. Pulmonary function test outcomes in patients with myopathies

Spirometry results in patients with myopathies (mean FVC upright 79 ± 10 % predicted; FVC supine 76 ± 10 % predicted) were lower than in healthy controls (mean FVC upright 106 ± 8 % predicted; FVC supine 102 ± 8 % predicted, both $p<0.0125$) (Table 1). FVC upright and FVC supine in patients with myopathies were not significantly different compared to Pompe patients. However, the mean postural drop between FVC upright and FVC supine (Δ FVC), indicating diaphragmatic weakness, was only 3 ± 4 % in patients with myopathies compared to 15 ± 12 % in patients with Pompe disease ($p=0.007$). Lastly, MEP was

Table 2
MRI outcomes.

	Myopathies (n=7)	Motor Neuron Diseases (n=5)	Pompe disease (n=35)	Healthy controls (n=18)
Lung volume ratio	2.19 ± 0.37	1.94 ± 0.29	2.37 ± 0.56	2.86 ± 0.53
Lung area ratio	2.13 ± 0.35	1.87 ± 0.31	2.22 ± 0.48	2.58 ± 0.39
Cranial-caudal ratio	1.55 ± 0.10*	1.43 ± 0.15	1.45 ± 0.24	1.72 ± 0.16
Anterior-posterior ratio	1.20 ± 0.09	1.15 ± 0.10	1.30 ± 0.11	1.26 ± 0.11
CC-AP ratio	1.30 ± 0.10**,^^	1.25 ± 0.13**,^	1.12 ± 0.18	1.37 ± 0.14
Diaphragm height ratio	1.17 ± 0.33	0.80 ± 0.17^^	1.28 ± 0.36	0.82 ± 0.24
Diaphragm area ratio	1.38 ± 0.47	0.82 ± 0.22^^	1.61 ± 0.64	0.90 ± 0.36

MRI outcomes are ratios, calculated by dividing the outcomes at end-inspiration by the outcomes at end-expiration, presented as means ± standard deviation. Differences between subgroups were calculated using multiple linear regression analysis, with adjustment for age, sex, smoking and forced vital capacity in upright position. Statistically significant differences between subgroups are indicated:
* p<0.05 compared to healthy controls.
** p<0.0125 compared to healthy controls.
^ p<0.05 compared to Pompe patients.
^^ p<0.0125 compared to Pompe patients.
CC-AP-ratio = cranial-caudal ratio divided by the anterior-posterior ratio.

lower in patients with myopathies (mean 54 ± 25) than in Pompe patients (mean 80 ± 27, p=0.048) (Table 1).

3.3. Pulmonary function test outcomes in patients with motor neuron diseases

In patients with motor neuron diseases FVC upright was 82 ± 14 % predicted and FVC supine was 79 ± 18 % predicted, both lower than in healthy controls (p<0.0125) and not significantly different from Pompe patients. No other pulmonary function test results in patients with motor neuron diseases were significantly different compared to healthy controls or Pompe patients.

3.4. MRI outcomes in patients with myopathies

In patients with myopathies, the mean cranial-caudal ratio (1.55 ± 0.10), evaluating the downwards motion of the diaphragm, was lower than in healthy controls (1.72 ± 0.16 (p=0.017)), but not significantly different compared to Pompe patients (1.45 ± 0.24) (Table 2). The anterior-posterior ratio, evaluating the motion of the thoracic wall, was similar in patients with myopathies, healthy controls and Pompe patients. Interestingly, the two patients with inclusion body myositis had a particularly low anterior-posterior ratio (Fig. 3C). The relative motion of the diaphragm compared to the motion of the thoracic wall (cranial-caudal ratio / anterior-posterior ratio), was 1.30 ± 0.10 in patients with myopathies versus 1.37 ± 0.14 in healthy controls (p=0.001) and 1.12 ± 0.1 in Pompe patients (p=0.011). This indicates a relative decreased diaphragmatic motion in patients with myopathies, but not as much as observed in patients with Pompe disease. In addition, in patients with myopathies the mean diaphragm height ratio was 1.17 ± 0.33 and the mean diaphragm area ratio was 1.38 ± 0.47. A ratio > 1 indicates an increasing diaphragmatic curvature during inspiration, which is similar to the ratios found in Pompe patients (1.28 ± 0.36 and 1.61 ± 0.64). Conversely, in healthy controls, these mean ratios are < 1 (0.82 ± 0.24 and 0.90 ± 0.36), indicating a decreasing curvature during inspiration (Fig. 2). Thus, the increased curvature reflects an insufficient contraction of the diaphragm during inspiration. Looking at the individual results, in particular the two patients with nemaline myopathy (Fig. 3D) and the patient with myofibrillar myopathy type 2 had an increased curvature of the diaphragm.

3.5. MRI outcomes in patients with motor neuron diseases

Similar to patients with myopathies, patients with motor neuron diseases had a decreased cranial-caudal ratio relative to the anterior-posterior ratio (mean 1.25 ± 0.13) compared to healthy controls (p=0.008), indicating that the function of the diaphragm is more impaired than the function of intercostal muscles (Fig. 2). However, opposite to patients with myopathies, the diaphragm height ratio (mean 0.80 ± 0.17) and diaphragm area ratio (mean 0.82 ± 0.22) were similar to healthy controls, suggesting a normal contraction of the diaphragm during inspiration (Fig. 3E and 3F). Both the diaphragm height ratio and diaphragm area ratio in patients with motor neuron diseases were lower than in Pompe patients (p=0.001 and p=0.002), meaning that the diaphragmatic curvature is more flat (Fig. 2).

3.6. Correlation between pulmonary function test outcomes and MRI outcomes

The correlation between pulmonary function test outcomes and MRI outcomes was moderate (Table 3). The ratio between the cranial-caudal ratio and the anterior-posterior ratio, evaluating the relative motion of the diaphragm compared to motion of the thoracic wall, showed the best correlation with FVC supine (ρ 0.509) and Δ FVC (ρ -0.572). Diaphragm height ratio, evaluating the curvature of the diaphragm, showed also the best correlation with FVC supine (ρ -0.597). Anterior-posterior ratio showed a weak correlation to all pulmonary function tests (ρ 0.009-0.240) and MEP showed a weak correlation to all MRI outcomes (ρ 0.113-0.271).

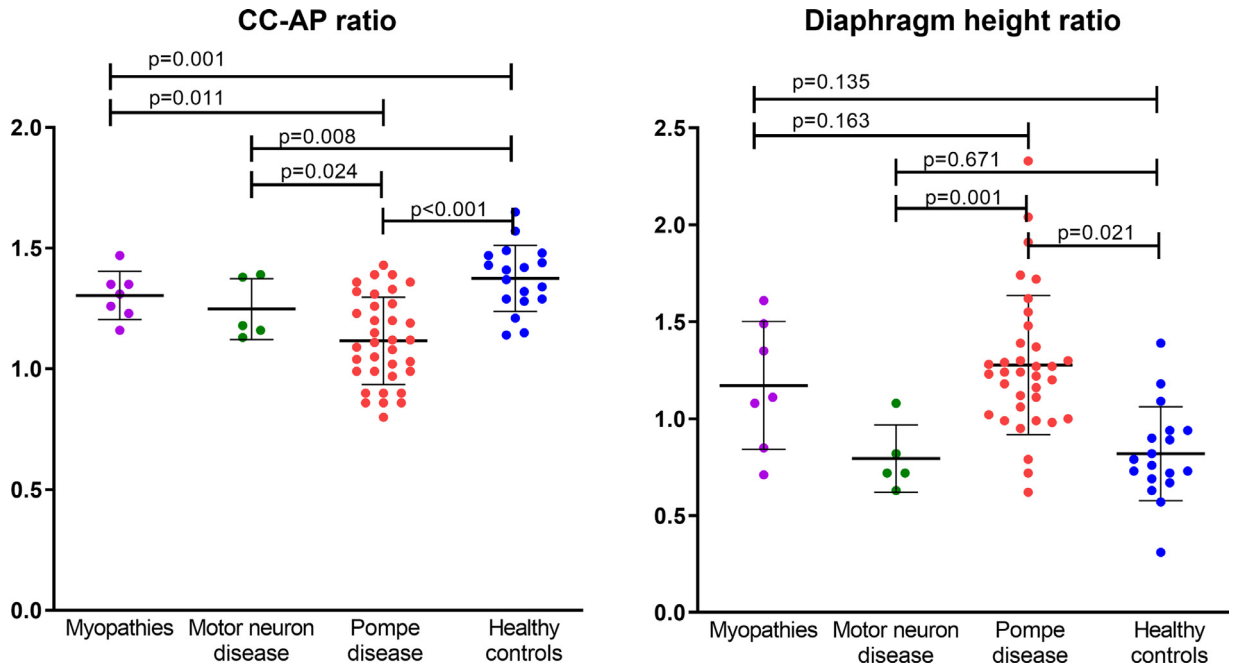

Fig. 2. Relative diaphragmatic motion and diaphragmatic curvature. Outcomes of diaphragmatic motion compared to motion of the thoracic wall (CC-AP ratio) and curvature of the diaphragm (diaphragm height ratio) in patients with other myopathies and motor neuron disease compared to Pompe patients and healthy controls. Error bars are means with standard deviations. Differences between subgroups, calculated using multiple linear regression analysis, with adjustment for age, sex, smoking and forced vital capacity in upright position, are indicated with p-values. CC-AP ratio = cranial-caudal ratio divided by the anterior-posterior ratio.

Table 3
Correlation between MRI outcomes and pulmonary function tests outcomes.

	FVC upright	FVC supine	Δ FVC	MIP	MEP
Lung volume ratio	0.532***	0.646***	-0.526***	0.371**	0.225
Lung area ratio	0.507***	0.626***	-0.462***	0.383**	0.221
Cranial-caudal ratio	0.414**	0.599***	-0.569**	0.386**	0.198
Anterior-posterior ratio	0.240	0.193	-0.009	0.095	0.113
CC-AP ratio	0.304*	0.509***	-0.572***	0.306*	0.119
Diaphragm height ratio	-0.460***	-0.597***	0.487***	-0.329**	-0.259*
Diaphragm area ratio	-0.476***	-0.587***	0.449***	-0.297*	-0.271*

Spearman correlation coefficients between MRI-outcomes (ratios between end-inspiration and end-expiration outcomes) and outcomes of pulmonary function tests (% predicted). Significant correlations are indicated with

* $p<0.05$.

** $p<0.01$.

*** $p<0.001$.

CC-AP ratio = cranial caudal ratio / anterior posterior ratio. FVC = forced vital capacity, Δ FVC = FVC upright - FVC supine, MEP = mean expiratory pressure, MIP = mean inspiratory pressure.

4. Discussion

In this exploratory study, we used spirometry-controlled MRI to study the involvement of respiratory muscles in various types of neuromuscular diseases. We found a decreased motion of the diaphragm relative to that of the thoracic wall in patients with myopathies as well as in patients with motor neuron diseases. This ratio was however decreased most in patients with Pompe disease, suggesting that Pompe patients had the most severe diaphragmatic involvement with a relatively preserved function of the intercostal muscles. Similar to Pompe patients, most patients with other myopathies also had a typical increased curvature of the diaphragm during inspiration, indicative for an insufficient diaphragmatic contraction. In patients with motor neuron diseases this curvature was within the normal range.

These results show that MRI can detect a disproportional involvement of diaphragmatic function compared to function of the intercostal muscles across patients with various types of neuromuscular disorders. The limited downwards motion and increased diaphragmatic curvature indicate diaphragmatic dysfunction, while the limited anterior motion of the thoracic wall likely indicates weakness of the intercostal muscles. However, the limited motion of the thoracic wall can also be caused by a decreased compliance due to

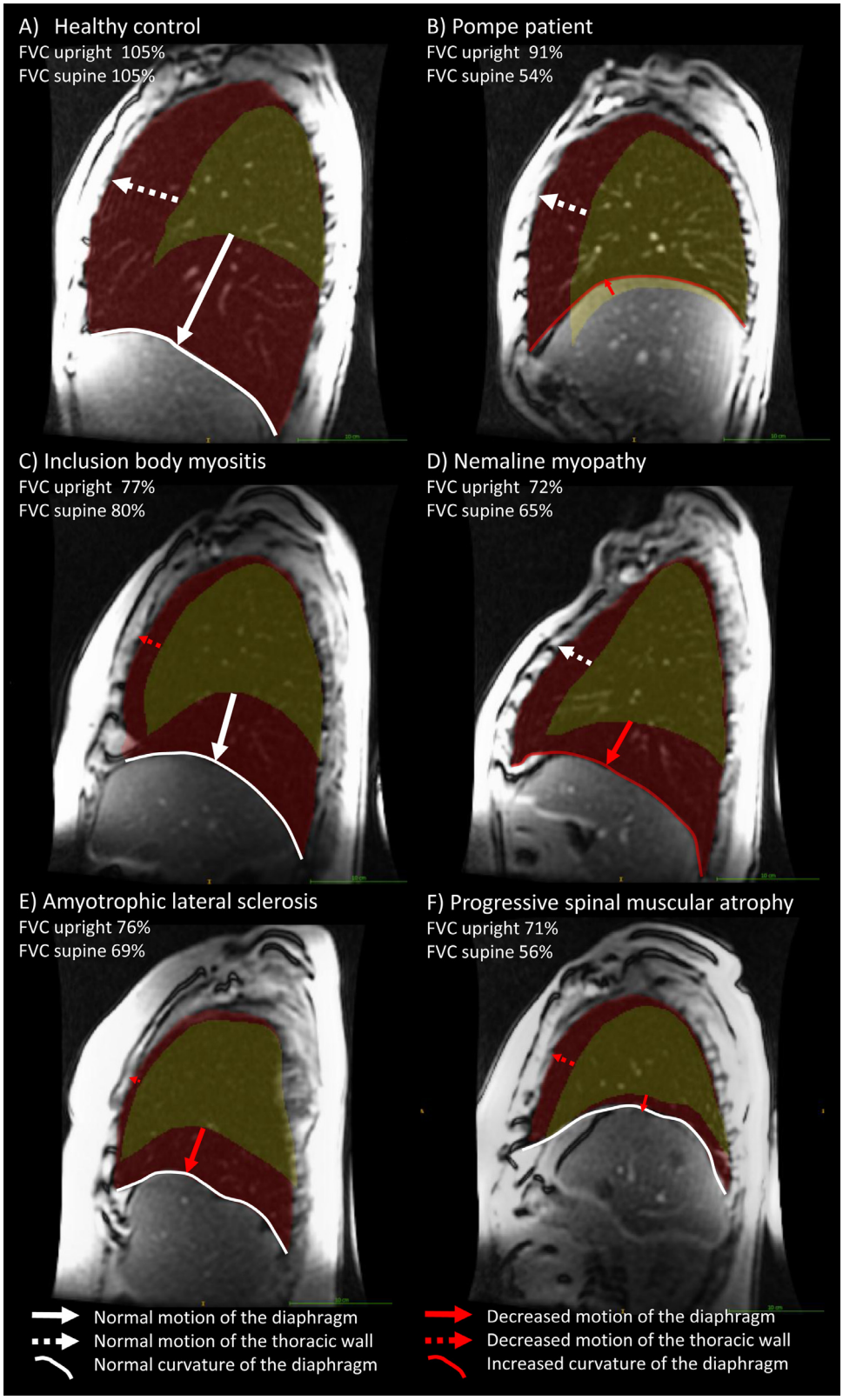

Fig. 3. Examples of different patterns of respiratory weakness. Sagittal images at end-inspiration in different neuromuscular diseases, compared to a healthy control (A). Red indicates the lung area in inspiration and yellow in expiration. The Pompe patient (B) has no downward motion of the diaphragm and an increased curvature of the diaphragm; motion of the thoracic wall is normal. The patient with inclusion body myositis (C) mainly had a decreased motion of the thoracic wall. The patient with nemaline myopathy (D) had a decreased motion of the diaphragm and an increased curvature of the diaphragm during inspiration. The patients with amyotrophic lateral sclerosis and progressive spinal muscular atrophy (E en F) had a decreased motion of both the diaphragm and the thoracic wall, but a normal curvature of the diaphragm.

increased stiffness of the chest or lung atelectasis [20]. The differentiation between diaphragmatic weakness and intercostal muscle weakness could not be made with routine pulmonary function tests such as forced vital capacity, that are commonly used as an indirect test to measure respiratory muscle function in patients with neuromuscular diseases in a clinical setting [21,22]. The moderate correlation between pulmonary function tests outcomes and MRI outcomes indicates that the results are supportive to each other, but also that MRI provides unique information about diaphragmatic function. Remarkably, in contrast to Pompe patients, neither patients with other myopathies nor patients with motor neuron disease in this study had a postural drop in forced vital capacity when moving from an upright position to a supine position, which is normally thought to be a good indicator of diaphragmatic weakness [23]. MRI can study the function of the diaphragm and that of the intercostal muscles independently and consequently indicate which respiratory muscles are involved. Moreover, MRI might be able to detect a decreased diaphragmatic function when pulmonary function tests are still in the normal range, as was previously illustrated in patients with Pompe disease [11]. Therefore MRI might be used to indicate early signs of diaphragmatic weakness in neuromuscular disease.

We also found some typical characteristics in individual patients with neuromuscular diseases. The increased diaphragmatic curvature that has been observed in Pompe disease, was also found in the patients with nemaline myopathy and myofibrillar myopathy type 2, in which respiratory difficulty is a known clinical feature [24–26]. This increased diaphragmatic curvature during inspiration might indicate an insufficient contraction of the diaphragm, which can possibly be explained by an impaired contraction of the sarcomeres caused by muscle fiber destruction with fatty infiltration and fibrosis in patients with myopathies [27–29]. A different pattern was observed in patients with motor neuron disease, who exhibit a normal curvature of the diaphragm during inspiration. We hypothesize that in these patients the curvature of the diaphragm may be normal, because despite atrophy of muscle fibers caused by denervation, the specific force of the remaining muscle fibers is normal caused by hypertrophic muscle fibers and a higher percentage of hybrid fibers [30–33]. Lastly, both patients with inclusion body myositis had a limited motion of the thoracic wall, suggesting involvement of intercostal muscles. Their relatively normal function of the diaphragm may be the reason why respiratory failure in these patients is rarely described and often remains asymptomatic [34–36].

In this study, we observed a decreased diaphragmatic motion and an insufficient diaphragmatic contraction in patients with neuromuscular disease using spirometer-controlled MRI. Although spirometer-controlled MRI is relatively expensive and time-consuming, it ensures the maximum performance of the patient during breathing maneuvers within the MRI. Previously, ultrasound demonstrated a decreased diaphragmatic thickness in patients with various myopathies and motor neuron diseases [37–40]. Ultrasound is easier to perform and less burdensome for patients than spirometry-controlled MRI. However, ultrasound requires an experienced operator to reduce observer variability [41]. In addition, simultaneous evaluation of the diaphragmatic motion and the thoracic wall motion, as well as evaluation of the curvature of the diaphragm, is not possible using ultrasound. Currently, it is unknown whether the decreased thickness found using ultrasound correlates to our MRI outcomes, and which outcome is most sensitive to detect early diaphragmatic weakness and progression of diaphragmatic weakness over time.

With the development of new therapies for neuromuscular diseases, accurate and sensitive outcome measures are needed to monitor disease progression and evaluate treatment effects. Also, early recognition of diaphragmatic weakness could be essential to start treatment in a timely manner to prevent possible irreversible damage to the diaphragm. Our results show that spirometry-controlled MRI is feasible in patients with myopathies and in patients with motor neuron disease. Our MRI outcomes might be used to detect early signs of diaphragmatic weakness and during follow-up. Whether evaluation of the diaphragmatic contraction during inspiration in patients with an unknown diagnosis, could help to differentiate between a myopathy or other causes of diaphragmatic weakness requires further investigation.

This study has some limitations. First, the number of patients we studied is limited and the group of patients is heterogeneous. This is related to the exploratory design of this study, aiming to gain more information on the involvement of the diaphragm and intercostal muscles across a variety of neuromuscular disorders. In order to study possible disease-specific patterns of muscle involvement, future studies would need a greater number of patients across a greater spectrum of each disease. Second, there were some differences in age, smoking habits and pulmonary function test results between the groups. Therefore, differences in MRI outcomes between groups were adjusted for these factors. Third, the analysis requires segmentations and measurements on dynamic MRI scans that would be time-consuming when done manually. We automated these steps with a computer algorithm, and showed that this is feasible across a group of patients with various neuromuscular diseases.

5. Conclusions

Using MRI, we were able to compare the function of the diaphragm to the function of the intercostal muscles across different types of neuromuscular disease. We observed that both in patients with myopathies and with motor neuron disease, the function of the diaphragm is particularly decreased. In addition, patients with myopathies seem to have an insufficient diaphragmatic contraction during inspiration. Our MRI findings warrant studies with larger cohorts of patients with neuromuscular diseases. This MRI technique holds promise as an assessment tool for the

sensitive evaluation of respiratory muscle weakness and potentially also for a better quantification of treatment responses.

Declaration of Competing Interest

Ans T. van der Ploeg has provided consulting services for various industries in the field of Pompe disease under an agreement between these industries and Erasmus MC, Rotterdam, The Netherlands. Harm A.W.M. Tiddens is director of the ErasmusMC LungAnalysis laboratory and acts as consultant for Thirona. All other authors report no relevant disclosures.

Acknowledgments

We thank prof. Dimitris Rizopoulos (Erasmus MC, University Medical Center Rotterdam, Department of Biostatistics) for help with the statistical analyses of the results. This work is supported by a grant from the Prinses Beatrix Spierfonds for neuromuscular disease (grant number W.OR15-10) and by ZonMw (grant number 0915016910230). Several of the authors of this publication are members of the European Reference Networks for Hereditary Metabolic Disorders (Metab-ERN) and Rare Neuromuscular Diseases (EURO-NMD).

References

[1] Gilchrist JM. Overview of neuromuscular disorders affecting respiratory function. Semin Respir Crit Care Med 2002;23:191–200.
[2] Boentert M, Wenninger S, Sansone VA. Respiratory involvement in neuromuscular disorders. Curr Opin Neurol 2017;30:529–37.
[3] Gayan-Ramirez G, Decramer M, et al. The Respiratory Muscles Fishman's Pulmonary Diseases and Disorders, 5e. Grippi MA, Elias JA, Fishman JA, Kotloff RM, Pack AI, Senior RM, et al., editors. New York: McGraw-Hill Education; 2015.
[4] Ratnovsky A, Elad D, Halpern P. Mechanics of respiratory muscles. Respir Physiol Neurobiol 2008;163:82–9.
[5] Harlaar L, Ciet P, van der Ploeg AT, Brusse E, van der Beek N, Wielopolski PA, et al. Imaging of respiratory muscles in neuromuscular disease: a review. Neuromuscul Disord 2018;28:246–56.
[6] Reuser AJJ, Hirschhorn R, Kroos MA. Pompe disease: glycogen storage disease type II, acid α-glucosidase (acid maltase) deficiency. The online metabolic and molecular bases of inherited disease. Valle DL, Antonarakis S, Ballabio A, Beaudet AL, Mitchell GA, editors. New York: McGraw-Hill Education; 2018.
[7] van der Beek NA, van Capelle CI, van der Velden-van Etten KI, Hop WC, van den Berg B, Reuser AJ, et al. Rate of progression and predictive factors for pulmonary outcome in children and adults with Pompe disease. Mol Genet Metab 2011;104:129–36.
[8] Wens SC, Ciet P, Perez-Rovira A, Logie K, Salamon E, Wielopolski P, et al. Lung MRI and impairment of diaphragmatic function in Pompe disease. BMC Pulm Med 2015;15:54.
[9] Mogalle K, Perez-Rovira A, Ciet P, Wens SC, van Doorn PA, Tiddens HA, et al. Quantification of Diaphragm Mechanics in Pompe Disease Using Dynamic 3D MRI. PLoS One 2016;11:e0158912.
[10] Gaeta M, Musumeci O, Mondello S, Ruggeri P, Montagnese F, Cucinotta M, et al. Clinical and pathophysiological clues of respiratory dysfunction in late-onset Pompe disease: New insights from a comparative study by MRI and respiratory function assessment. Neuromuscular Disord 2015;25:852–8.
[11] Harlaar L, Ciet P, van Tulder G, Pittaro A, van Kooten HA, van der Beek NAME, et al. Chest MRI to diagnose early diaphragmatic weakness in Pompe disease. Orphanet J Rare Dis 2021;16:21.
[12] Barnard AM, Lott DJ, Batra A, Triplett WT, Forbes SC, Riehl SL, et al. Imaging respiratory muscle quality and function in Duchenne muscular dystrophy. J Neurol 2019;266:2752–63.
[13] Bishop CA, Ricotti V, Sinclair CDJ, Evans MRB, Butler JW, Morrow JM, et al. Semi-automated analysis of diaphragmatic motion with dynamic magnetic resonance imaging in healthy controls and non-ambulant subjects with duchenne muscular dystrophy. Front Neurol 2018;9:9.
[14] Pennati F, Arrigoni F, LoMauro A, Gandossini S, Russo A, D'Angelo MG, et al. Diaphragm involvement in Duchenne muscular dystrophy (DMD): an MRI study. J Magn Reson Imaging 2020;51:461–71.
[15] American Thoracic Society/European Respiratory SocietyATS/ERS Statement on respiratory muscle testing. Am J Respir Crit Care Med 2002;166:518–624.
[16] Quanjer PH, Stanojevic S, Cole TJ, Baur X, Hall GL, Culver BH, et al. Multi-ethnic reference values for spirometry for the 3-95-yr age range: the global lung function 2012 equations. Eur Respir J 2012;40:1324–43.
[17] Wilson SH, Cooke NT, Edwards RH, Spiro SG. Predicted normal values for maximal respiratory pressures in caucasian adults and children. Thorax 1984;39:535–8.
[18] Ronneberger O, Fischer P, Brox T. U-net: convolutional networks for biomedical image segmentation. Medical image computing and computer-assisted intervention – MICCAI 2015. Navab N, Hornegger J, Wells W, Frangi A, editors. Springer, Cham; 2015. MICCAILecture Notes in Computer Science, vol 9351.
[19] Tustison NJ, Avants BB, Cook PA, Zheng Y, Egan A, Yushkevich PA, et al. N4ITK: improved N3 bias correction. IEEE Trans Med Imaging 2010;29:1310–20.
[20] Kennedy JD, Martin AJ. Chronic respiratory failure and neuromuscular disease. Pediatr Clin North Am 2009;56:261–73 xii.
[21] Pirola A, De Mattia E, Lizio A, Sannicolo G, Carraro E, Rao F, et al. The prognostic value of spirometric tests in Amyotrophic Lateral Sclerosis patients. Clin Neurol Neurosurg 2019;184:105456.
[22] Pinto S, de Carvalho M. Comparison of slow and forced vital capacities on ability to predict survival in ALS. Amyotroph Lateral Scler Frontotemporal Degener 2017;18:528–33.
[23] Fromageot C, Lofaso F, Annane D, Falaize L, Lejaille M, Clair B, et al. Supine fall in lung volumes in the assessment of diaphragmatic weakness in neuromuscular disorders. Arch Phys Med Rehabil 2001;82:123–8.
[24] Selcen D. Myofibrillar myopathies. Neuromuscul Disord 2011;21:161–71.
[25] Ryan MM, Schnell C, Strickland CD, Shield LK, Morgan G, Iannaccone ST, et al. Nemaline myopathy: a clinical study of 143 cases. Ann Neurol 2001;50:312–20.
[26] Sanoudou D, Beggs AH. Clinical and genetic heterogeneity in nemaline myopathy–a disease of skeletal muscle thin filaments. Trends Mol Med 2001;7:362–8.
[27] Jungbluth H, Treves S, Zorzato F, Sarkozy A, Ochala J, Sewry C, et al. Congenital myopathies: disorders of excitation-contraction coupling and muscle contraction. Nat Rev Neurol 2018;14:151–167.
[28] Romero NB, Clarke NF. Congenital myopathies. Handb Clin Neurol 2013;113:1321–36.
[29] van Adel BA, Tarnopolsky MA. Metabolic myopathies: update 2009. J Clin Neuromuscul Dis 2009;10:97–121.
[30] Turner MR, Swash M. The expanding syndrome of amyotrophic lateral sclerosis: a clinical and molecular odyssey. J Neurol Neurosurg Psychiatry 2015;86:667–73.
[31] Pansarasa O, Rossi D, Berardinelli A, Cereda C. Amyotrophic lateral sclerosis and skeletal muscle: an update. Mol Neurobiol 2014;49:984–90.

[32] Baloh RH, Rakowicz W, Gardner R, Pestronk A. Frequent atrophic groups with mixed-type myofibers is distinctive to motor neuron syndromes. Muscle Nerve 2007;36:107–10.
[33] Krivickas LS, Yang JI, Kim SK, Frontera WR. Skeletal muscle fiber function and rate of disease progression in amyotrophic lateral sclerosis. Muscle Nerve 2002;26:636–43.
[34] Voermans NC, Vaneker M, Hengstman GJ, ter Laak HJ, Zimmerman C, Schelhaas HJ, et al. Primary respiratory failure in inclusion body myositis. Neurology 2004;63:2191–2.
[35] Cohen R, Lipper S, Dantzker DR. Inclusion body myositis as a cause of respiratory failure. Chest 1993;104:975–7.
[36] Rodríguez Cruz PM, Needham M, Hollingsworth P, Mastaglia FL, Hillman DR. Sleep disordered breathing and subclinical impairment of respiratory function are common in sporadic inclusion body myositis. Neuromuscul Disord 2014;24:1036–41.
[37] Sartucci F, Pelagatti A, Santin M, Bocci T, Dolciotti C, Bongioanni P. Diaphragm ultrasonography in amyotrophic lateral sclerosis: a diagnostic tool to assess ventilatory dysfunction and disease severity. Neurol Sci 2019;40:2065–71.
[38] Pinto S, Alves P, Pimentel B, Swash M, de Carvalho M. Ultrasound for assessment of diaphragm in ALS. Clin Neurophysiol 2016;127:892–7.
[39] Laviola M, Priori R, D'Angelo MG, Aliverti A. Assessment of diaphragmatic thickness by ultrasonography in Duchenne muscular dystrophy (DMD) patients. PLoS One 2018;13:e0200582.
[40] O'Gorman CM, O'Brien TG, Boon AJ. Utility Of diaphragm ultrasound in myopathy. Muscle Nerve 2017;55:427–9.
[41] Cappellini I, Picciafuochi F, Bartolucci M, Matteini S, Virgili G, Adembri C. Evaluation of diaphragm thickening by diaphragm ultrasonography: a reproducibility and a repeatability study. J Ultrasound 2020.